Schizophrenia Bulletin vol. 45 no. 3 pp. 659–669, 2019
doi:10.1093/schbul/sby077
Advance Access publication 7 June 2018

Dynamic Reorganization of Functional Connectivity Reveals Abnormal Temporal Efficiency in Schizophrenia

Yu Sun*[,1,2], Simon L. Collinson[3], John Suckling[4], and Kang Sim [5,6]

[1]Key Laboratory for Biomedical Engineering of Ministry of Education, Department of Biomedical Engineering, Zhejiang University, Zhejiang, China; [2]Centre for Life Sciences, National University of Singapore, Singapore; [3]Department of Psychology, Faculty of Arts & Social Sciences, National University of Singapore, Singapore; [4]Brain Mapping Unit, Department of Psychiatry, School of Clinical Medicine, Herchel Smith Building for Brain and Mind Sciences, University of Cambridge, Cambridge, United Kingdom; [5]Department of General Psychiatry, Institute of Mental Health (IMH), Singapore; [6]Department of Research, Institute of Mental Health (IMH), Singapore

*To whom correspondence should be addressed; Key Laboratory for Biomedical Engineering of Ministry of Education, Department of Biomedical Engineering, Zhejiang University, 310000, Zhejiang, China; tel: +86-18321575735, fax: +86-57187951676, e-mail: yusun@zju.edu.cn.

Emerging evidence suggests that schizophrenia is associated with brain dysconnectivity. Nonetheless, the implicit assumption of stationary functional connectivity (FC) adopted in most previous resting-state functional magnetic resonance imaging (fMRI) studies raises an open question of schizophrenia-related aberrations in dynamic properties of resting-state FC. This study introduces an empirical method to examine the dynamic functional dysconnectivity in patients with schizophrenia. Temporal brain networks were estimated from resting-state fMRI of 2 independent datasets (patients/controls = 18/19 and 53/57 for self-recorded dataset and a publicly available replication dataset, respectively) by the correlation of sliding time–windowed time courses among regions of a predefined atlas. Through the newly introduced temporal efficiency approach and temporal random network models, we examined, for the first time, the 3D spatiotemporal architecture of the temporal brain network. We found that although prominent temporal small-world properties were revealed in both groups, temporal brain networks of patients with schizophrenia in both datasets showed a significantly higher temporal global efficiency, which cannot be simply attributable to head motion and sampling error. Specifically, we found localized changes of temporal nodal properties in the left frontal, right medial parietal, and subcortical areas that were associated with clinical features of schizophrenia. Our findings demonstrate that altered dynamic FC may underlie abnormal brain function and clinical symptoms observed in schizophrenia. Moreover, we provide new evidence to extend the dysconnectivity hypothesis in schizophrenia from static to dynamic brain network and highlight the potential of aberrant brain dynamic FC in unraveling the pathophysiologic mechanisms of the disease.

Key words: dynamic functional connectivity/resting-state fMRI/dysconnectivity/spatiotemporal disorganization/temporal efficiency

Introduction

Schizophrenia is a complex neuropsychiatric disorder with a myriad of clinical manifestations.[1] While the precise neural substrates underpinning the heterogeneous clinical manifestations are far from understood, it is increasingly being conceptualized as a disorder that results from abnormal interactions between brain regions,[2–5] coinciding with the recent advent of human connectome studies.[6,7] For instance, a number of resting-state functional magnetic resonance imaging (fMRI) studies showed widespread dysconnectivity,[3] which leads to aberrant network topology in schizophrenia, including reduced local clustering/efficiency[8–10] and modularity (an optimal partition of a brain network into smaller functional communities),[11,12] as well as increased global integration[10,11,13] and network robustness (under targeted and/or random node removal).[13] However, most of the aforementioned resting-state functional connectivity (FC) studies were performed in a static manner with an implicit assumption of stationary FC during the scanning period,[14,15] while accumulating evidences have suggested that brain networks are dynamically connected and quantifying dynamic FC may provide new insights into fundamental properties of brain networks.[16–18]

It is noteworthy that the investigation of dynamic FC in schizophrenia is only beginning to be revealed. Using a sliding-window approach, Sakoğlu et al[19] investigated the resting-state dynamic FC and found significant

aberrations in the time–frequency patterns of dynamic FC in patients with schizophrenia. Through further clustering the dynamic FC into a set of connectivity states (recurring connectivity patterns), Damaraju et al[20] showed that healthy participants switched more often among the states in comparison with a rigid dynamic FC pattern in schizophrenic patients. Similar observation was also evidenced in other works.[21,22] Meanwhile, to delineate the architecture of the aberrant dynamic FC, graph theoretical analysis was applied separately to network within each sliding window.[18,23–25] Through inspecting the variance of the obtained graph measures, Du et al[25] found schizophrenia-related aberrant global and local properties of the dynamic FC states within default mode network. Extending this framework to the whole brain, the same metrics were found to be lower and less fluctuant in patients with schizophrenia.[26] Beyond the simplistic stationary characterization, these studies have provided some of the first quantitative insights to unveil aberrant flexibility in the functional coordination between different neural systems in schizophrenia.

To date, no study has investigated the combined 3D spatiotemporal architecture of the whole temporal brain network (ie, the spatiotemporal distribution of dynamic FC) in terms of information flow in patients with schizophrenia. Given the known dynamic nature of brain activity and connectivity,[16–18] we believe that examining the topological characteristics of dynamic FC may lead to a better understanding of fundamental properties of brain function in behavioral shifts and adaptive processes, and potentially help to elucidate the etiology of schizophrenia. In this study, we used our newly developed analysis framework[27] (1) to delineate temporal small-world properties of dynamic FC using resting-state fMRI data, and (2) to provide a clear and direct physical meaning to the concept of 3D spatiotemporal architecture concerning efficiency of information flow for quantitatively assessing dynamic reorganization of FC in schizophrenia. On the basis of the consistent observations of small-world architecture in static brain networks,[6] we hypothesized that temporal brain networks of both groups would exhibit prominent temporal small-world topology. Moreover, On the basis of convergent findings of a subtle randomization in static brain network architecture[14,15] as well as aberrant dynamic FC patterns in schizophrenia,[19–21,25,26,28] we further hypothesized that schizophrenic patients would show a more randomized spatiotemporal distribution of dynamic FC in comparison with healthy volunteers.

Methods and Materials

Subjects

Two independent datasets were included: *a self-recorded dataset* of 20 patients with a *Diagnostic and Statistical Manual of Mental Disorders*, Fourth Edition diagnosis of schizophrenia and 20 matched healthy volunteers recruited from the Institute of Mental Health (IMH), Singapore, and local community through advertisements. The detailed inclusion and exclusion criteria are described in Supplementary materials. The protocol of the study was approved by the institutional review boards of the IMH and written informed consent was obtained from each participant. *A publicly available dataset* (COBRE, http://fcon_1000.projects.nitrc.org/indi/retro/cobre.html) of 72 patients and 75 healthy volunteers was used as an independent replication dataset.

Data Acquisition

Self-recorded Dataset. All subjects underwent a resting-state MRI scan using a 3 Tesla scanner (Philips Achieva) at National Neuroscience Institute, Singapore. One high-resolution T1-weighted MRI and one resting-state fMRI (8 min) were acquired.

Publicly Available Dataset. The replication dataset was acquired with a 3 Tesla Siemens Trio scanner (Siemens, Germany) and included a high-resolution T1-weighted images and resting-state fMRI scan (5 min).

For the details of scanning parameters, see Supplementary materials.

Data Preprocessing

We used the DPARSF toolbox (http://rfmri.org/DPARSF)[29] to carry out data preprocessing, which include removal of first 10 volumes, slice-time correction, head motion correction, anatomical coregistration, new segmentation to DARTEL,[30] nuisance signal regression, spatial normalization, and bandpass filtering. Of note, the data of 1 healthy participant and 2 patients in the principal dataset and 18 healthy controls and 19 patients in the replication dataset were discarded due to significant head motion.[31] For demographics of the included subjects, see table 1. Greater details of the resting-state fMRI data preprocessing and criteria for significant head motion are provided in Supplementary materials.

Temporal Network Construction

A widely used sliding-window approach[34–36] was applied on the time series, which were extracted from the estimation of mean values of voxels within a region of interest (ROI). Here, a previously validated atlas[37] was used to parcellate the brain into 90 ROIs. The names and corresponding abbreviations of the cortical regions were listed in supplementary table 1. The Pearson's correlation coefficient between all pairs of the time series was taken as the level of functional coupling.[38] A schematic diagram of the temporal network construction is shown in supplementary figure S1. Here, the window length was chosen as 100 s with an incremental step of 6 s to balance the dynamics of the BOLD signals and the quality of connectivity estimation,

Table 1. Demographic and Clinical Characteristics of the Samples[a]

Characteristics	Self-recorded Dataset		Publicly Available Replication Dataset (COBRE)	
	Patients (n = 18)	Controls (n = 19)	Patients (n = 53)	Controls (n = 57)
Age (y)	24–56 (38.8 ± 9.9)	28–59 (37.7 ± 9.0)	18–65 (38.3 ± 13.9)	18–62 (35.4 ± 11.9)
Gender: male/female	10/8	10/9	41/12	37/20
Handedness: R/L/A	17/1/0	19/0/0	44/8/1	55/1/1[†]
Education (y)	6–16 (11.2 ± 3.1)	10–19 (15.1 ± 2.2)[b,*]	10–20 (13.1 ± 1.8)[c]	12–17 (14.0 ± 1.6)[d,*]
Age of onset (y)	17–47 (26.2 ± 8.3)	—	5–61 (22.7 ± 9.4)	—
Duration of illness (y)	1–30 (11.6 ± 8.4)	—	0–47 (15.6 ± 12.0)	—
Medication dose[e] (mg/day)	50–850 (293.9 ± 214.1)	—	0–1800 (368.7 ± 310.8)	—
PANSS symptoms[f]				
Positive symptoms	7–14 (9.5 ± 2.8)	—	7–28 (15.1 ± 4.9)	—
Negative symptoms	7–26 (10.9 ± 5.2)	—	8–29 (13.8 ± 4.0)	—
General symptoms	16–28 (20.0 ± 3.5)	—	16–56 (29.9 ± 8.5)	—
Overall symptoms	30–53 (40.4 ± 7.1)	—	35–94 (59.8 ± 14.0)	—
Global assessment of functioning				
Total	31–70 (49.7 ± 10.7)	—	—	—
Symptoms	31–71 (53.1 ± 13.1)	—	—	—
Disability	31–70 (51.3 ± 10.3)	—	—	—

Note: R, right; L, left; A, ambidextrous—within each dataset; *indicates significant ($P < 0.05$) between-group difference in a 2-sample 2-tailed t-test; †indicates significant ($P < 0.05$) between-group difference via a 2-tailed Pearson χ^2 test. Detailed statistics could be found in the supplementary table S2 (for self-recorded dataset) and table S3 (for publicly available replication dataset).
[a]Unless otherwise indicated, data are expressed as a range of minimum – maximum (mean ± SD).
[b]Data were missing for 1 normal control in the principal dataset.
[c]Data were missing for 3 patients with schizophrenia in the replication dataset.
[d]Data were missing for 7 normal controls in the replication dataset.
[e]The antipsychotic medication dosage was converted to daily chlorpromazine milligram equivalents according to Woods.[32] Detailed medical types could be found in supplementary table S2.
[f]The Positive and Negative Syndrome Scale (PANSS)[33] was used to assess the psychopathology and symptom severity.

as well as to reduce the computational complexity.[39,40] As such, one temporal network $G^w = \{G_t^w\}_{t=1,2,3,\cdots,T}$, where G_t^w is a static weighted graph within each window and T is the lifetime ($T = 60$ for self-recorded dataset and $T = 30$ for the replication dataset) obtained for each participant. Detailed steps for temporal network construction are shown in Supplementary materials.

Temporal Efficiency Analysis

Before the network analysis, each of the obtained temporal networks was thresholded into a binarized matrix (G_t) with a commonly applied sparsity approach to ensure that the assessment of intrinsic between-group differences in the topological architecture of the temporal networks without bias from different number of contacts and possible inclusion of low-weight spurious connections.[41,42] Here, a range of sparsity (0.5%–10%) with an interval 0.25% was selected to retain the most prominent dynamic FC (backbone). Threshold values for the inclusion of dynamic FC are shown in supplementary figure S2(A). Detailed criteria for sparsity selection were shown in Supplementary materials. Examples of the obtained binary temporal brain network are presented in figure 1 and the Supplementary video.

Once we obtained the binarized network, we could estimate the temporal distance $(\tau_{i\to j}(t)) : \tau_{i\to j}(t)$ defined as the smallest number of time steps required to reach node j from node i starting at time t (supplementary figure S3).[27,43] Of note, a temporal distance can be any positive integer, with the smallest value being 1 (when i and j are connected through a static path at time t) and the largest value being infinity (when no time-respecting path exists from i to j at time t). It is noteworthy that temporal distance is a measure in the time domain, which is influenced by both the topology of each of the snapshot static graphs and the temporal structure of the network.

Based on the estimation of temporal distances, we then investigated the 3D spatiotemporal architecture of the temporal brain network using a unified efficiency approach,[27] that is, the global network topology was quantified in terms of temporal global efficiency (E^t_{glob}) and temporal local efficiency (E^t_{loc}). Heuristically, one can regard E^t_{glob} as a measure of the overall information transfer efficiency in a temporal network, whereas the E^t_{loc} as a measure of the resilience of the temporal network to local failures. Regional properties were described in terms of temporal nodal efficiency ($E^t_{nodal}(G, i)$). In Appendix, we provided a brief glossary of concepts, whereas greater details of the formulation and interpretation of these metrics could be found in Supplementary materials or our previous methodological work.[27]

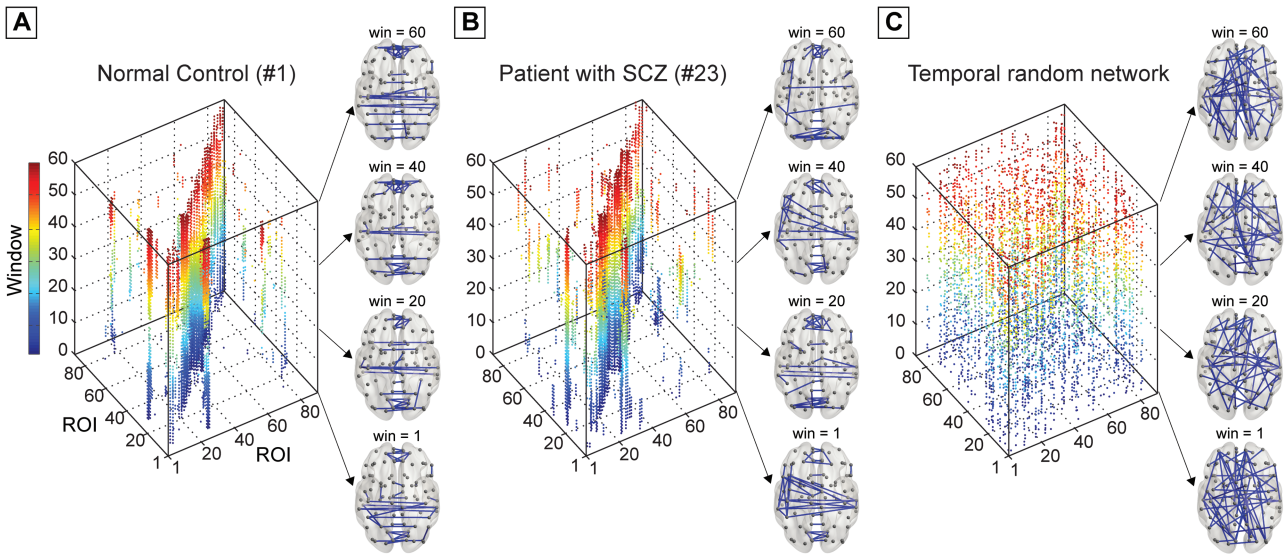

Fig. 1. Examples of temporal brain networks of (A) one normal control and (B) one patient randomly selected from each group. The example temporal brain networks are obtained using a fixed sparsity of 1%. The corresponding temporal random reference network is presented (C). The spatial distributions of the dynamic functional connections are also presented in the right panel at [1, 20, 40, 60] windows (see all windows in Supplementary video). The dynamic functional connections within each window/snapshot are color-coded with the color bar representing the corresponding temporal window.

Temporal Reference Network

The richness of the complex structures in temporal networks allows the application of powerful temporal randomization techniques,[44–46] which could be used to produce reference networks for temporal small-world topology identification. A 2-step randomization approach was implemented in the current: first, we employed randomized edges[46] technique to destroy the topological structure of the aggregated graph of temporal network, while preserving the distribution of the contact sequences, the total number of contacts, and the connectedness of the aggregated network. Second, to further randomize the temporal network in terms of contact sequences, the obtained topologically randomized temporal networks were subjected to randomized contacts technique to randomly redistribute the contacts among all connected node pairs.[27] An example of temporal random network is shown in figure 1C. Following the small-world definition in static network,[47] a real temporal network would be considered temporally small-world if it meets the following criteria: $E^t_{loc}/E^t_{loc\_rand} >> 1$ and $E^t_{glob}/E^t_{glob\_rand} \approx 1$. Here, $E^t_{loc\_rand}$ and $E^t_{glob\_rand}$ are the mean overall temporal global efficiency and temporal local efficiency estimated from 100 temporal random networks. Details on the temporal reference network construction are shown in Supplementary materials.

Statistical Analysis

To reduce the dependency of any significant differences in the network topology on the arbitrary choice of a single-threshold selection, an integrated network metric was estimated over the predefined sparsity range.[41] Separate nonparametric permutation test[48] with 100 000 iterations was used to investigate the differences of the temporal efficiencies between both groups. A value of $P < 0.05$ was considered significant. Corrections for multiple comparisons of regional characteristics were performed via false discovery rate (FDR) at $q = 0.05$.

Multiple linear regressions were used to assess the association between the network metrics and clinical variables in the patient group. To limit the number of association calculations for regional properties, only network metrics that displayed significant between-group different were chosen as independent variables. Statistical analyses were performed using SPSS 17. Further details of statistical analysis are provided in Supplementary materials.

Validation Analysis

To validate the reproducibility of our results, we adopted 2 procedures as follows:

Regional Parcellation Effects. Recent neuroimaging studies have showed that different parcellation schemes might lead to different properties of brain networks.[49,50] To assess the effect of different parcellation schemes and to provide more comprehensive information, 2 additional widely used parcellation schemes (ie, the Harvard-Oxford Atlas (HOA-112)[51,52] and the Craddock's functional atlas (Craddock-200)[53]) (supplementary figure S4) were adopted. The network construction procedures and temporal network analysis approaches were repeated for both templates.

Temporal Network Construction. Recent studies of dynamic FC showed that sliding-window correlation might be influenced by the window length and a range between 40 and 100 s was recommended.[34,40,54] Here, to validate our main observations in terms of different settings of temporal network construction, we performed the same analysis with different temporal window length and step length (window/step = [40, 60, 80, 100]/[2, 4, 6] s). Given that consistent findings were revealed across different settings (supplementary table S6), the less computational complexity combination of window/step = 100/6 s was chosen to present the main findings.

Results

Temporal Small-World Properties

The brain networks of both groups in the self-recorded dataset exhibited typically temporal small-world properties (supplementary figure S5), suggesting that temporal evolution and topologic arrangement of the temporal brain network permits effective coordination of various brain regions for globally integrated brain functions and efficient information transfer over time among neighboring brain regions for temporal functional specialization.

Additional quantitative statistical analyses revealed significantly higher temporal global efficiency ($P = 0.033$, 100 000 permutations) in patients with schizophrenia (figure 2A). We performed additional analyses to account for the potential confounding effects of age, gender, years of educations, medication dosage, head motion (via mean framewise displacement (FD) values), and overall strength of FC on the observed between-group differences. These confounds were included as linear regressors and the differences of the residuals between both groups were assessed again using permutation test. Results indicated that the reported higher E^t_{glob} were not explained by variance related to any of these factors. In line with the self-recorded dataset, a significantly higher temporal global efficiency was observed in patients group ($P = 0.029$) in the publicly available dataset (supplementary figure S6, supplementary table S4).

Moreover, in our validation analysis of the reproducibility, we found the same schizophrenia-related disruption of temporal global efficiency that is independent of parcellation schemes (supplementary table S5) and settings for temporal network construction (supplementary table S6). Taken together, these verification results lead us to believe that the observed between-group differences in E^t_{glob} may represent an intrinsic schizophrenia-related aberration in dynamic FC.

Abnormal Temporal Regional Properties

In the self-recorded dataset, schizophrenia-related significant increment ($P < 0.05$, FDR-corrected) of temporal regional efficiency was revealed in 18 regions across the cerebral cortex (including the left inferior gyrus, opercula, and triangular parts [IFGoperc.L, IFGtriang.L]; left orbitofrontal gyrus, inferior part [ORBinf.L]; left postcentral gyrus [PoCG.L]; left middle occipital gyrus [MOG.L]; left temporal pole, middle part [TPOmid.L]; right caudate nucleus [CAU.R]; right precuneus [PCUN.R]; right cuneus [CUN.R]; right lingual gyrus [LING.R];and bilaterally in amygdala [AMYG]; parahippocampal gyrus [PHG]; pallidium [PAL]; and putamen [PUT]), where most of these regions were resided in the left inferior frontal, right medial parietal, and bilateral subcortical areas (figure 3).

In the publicly available dataset, significantly higher ($P < 0.05$, FDR-corrected) temporal regional efficiency was found in the left IFGtring, the left ORBinf, the left hippocampus, [HIP.L], bilateral PHG, bilateral CAU,

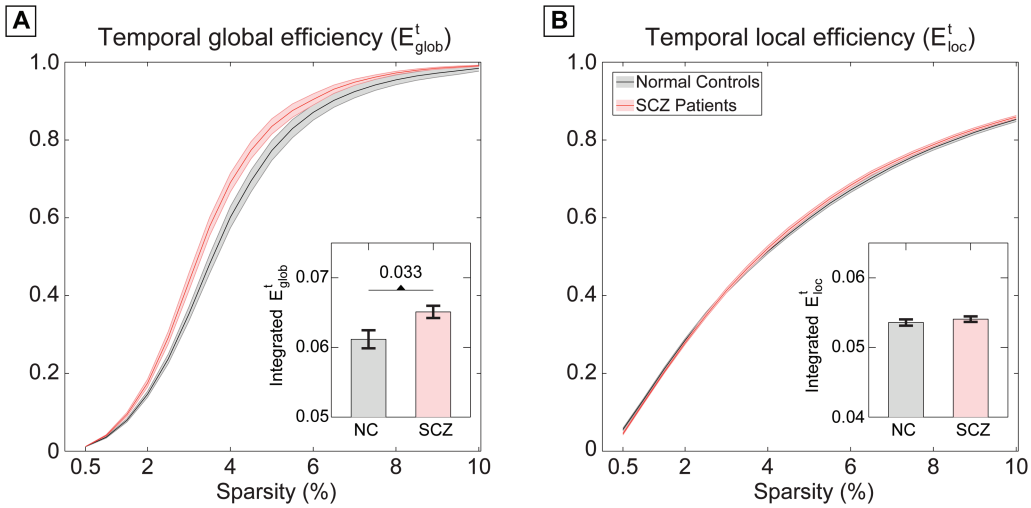

Fig. 2. (A) Temporal global efficiency and (B) temporal local efficiency of the dynamic functional connectivity as a function of sparsity in the self-recorded dataset. The integrated temporal efficiency measures (over the entire sparsity range) are shown at the bottom of the corresponding plot (bars represent mean ± SEM).

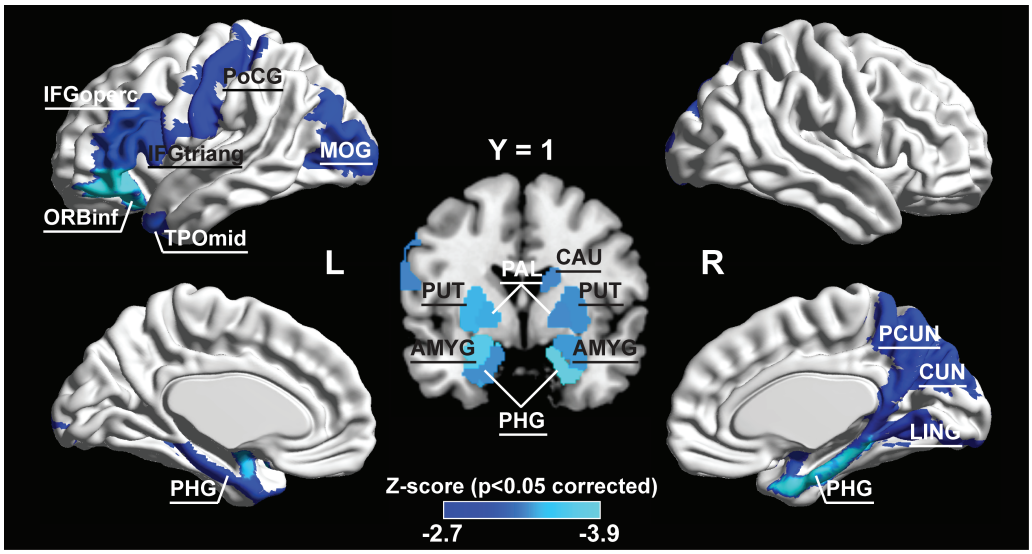

Fig. 3. The spatial distribution of cortical regions showing significant between-group difference ($P < 0.05$, FDR (false discovery rate)-corrected) in the self-recorded dataset. The color bar represents Z-score. For the abbreviations of the cortical regions, see supplementary table 1. L = left, R = right.

bilateral TPOmid, and bilateral inferior temporal gyrus [ITG] (supplementary figure S7), which were largely overlapped with the regional findings in the self-recorded dataset.

Relationship Between Temporal Efficiency Metrics and Clinical Features

In the self-recorded dataset, 7 regions exhibited significant correlations with the clinical measurements. Specifically, a significant positive correlation was observed between the temporal regional efficiency in the ORBinf.L and positive symptoms ($r = 0.603$, $P = 0.023$) on the Positive and Negative Syndrome Scale (PANSS). For the PANSS-negative symptoms, significant negative correlations were found in the AMYG.R ($r = -0.705$, $P = 0.004$), CUN.R ($r = -0.581$, $P = 0.029$), LING.R ($r = -0.532$, $P = 0.047$), MOG.L ($r = -0.642$, $P = 0.013$), PCUN.R ($r = -0.802$, $P < 0.001$ *, * indicates correlation-survived FDR threshold at $q < 0.05$), and TPOmid.L ($r = -0.711$, $P = 0.004$ *). For the PANSS-general symptoms, a significant positive relationship was found in the ORBinf.L ($r = 0.620$, $P = 0.018$). For the PANSS-overall symptoms, only AMYG.R ($r = -0.678$, $P = 0.007$) and TPOmid.L ($r = -0.562$, $P = 0.036$) exhibited significant negative correlation (table 2).

In the replication dataset, relationship between temporal network metrics and clinical variables failed to pass the significance threshold ($P > 0.05$).

Discussion

We report a functional neuroimaging analysis examining the schizophrenia-related dynamic functional dysconnectivity. To our knowledge, this is the first study to directly examine the 3D spatiotemporal architecture of the temporal brain networks in patients with schizophrenia. The significant findings are as follows: first, although the optimal temporal small-world properties were preserved, a significantly higher temporal global efficiency was revealed in patients; second, we found prominently localized changes of the temporal nodal properties in the left frontal, right medial parietal, and bilateral subcortical areas; third, the aberration of temporal network topological properties was correlated with the clinical features of schizophrenia.

The temporal brain network in patients with schizophrenia exhibited a significantly higher temporal global efficiency with a preserved temporal local efficiency, indicating a tendency toward a more random organization of temporal brain networks (supplementary figure S5). Of note, a subtle randomization of functional network architecture has been repeatedly reported in static FC studies of schizophrenia.[10,14] In searching for the origin of such topological alterations, 2 recent studies showed more spatially diverse static FC in patients with schizophrenia.[13,55] Taking into account time-varying role of dynamic FC, our findings may therefore extend this finding to a context of spatiotemporal randomization of temporal brain network architecture in schizophrenia. Heuristically, the higher temporal global efficiency, the shorter temporal distances between pairs of nodes in the temporal network.[44,46] The finding of higher temporal global efficiency therefore represents more fluctuations of the dynamic brain network backbone in schizophrenia (see an example in Supplementary video). However, our findings are unlike recent studies of dynamic dysconnectivity in schizophrenia,[25,26] which revealed low fluctuations of brain network metrics.

Table 2. Partial Correlation Coefficients Between Temporal Network Metrics and Clinical Characteristics of Patients with Schizophrenia in the Self-Recorded Dataset

	Partial Correlation Coefficients (*P* Value)				
Metrics	Duration	PANSS Positive	PANSS Negative	PANSS General	PANSS Overall
E^t_{nodal}(ORBinf.L)	−0.287 (0.320)	**0.603 (0.023)**	−0.204 (0.484)	**0.620 (0.018)**	0.407 (0.149)
E^t_{nodal}(AMYG.R)	−0.206 (0.479)	−0.126 (0.668)	**−0.705 (0.004)**	−0.371 (0.191)	**−0.678 (0.007)**
E^t_{nodal}(CUN.R)	−0.099 (0.736)	0.454 (0.103)	**−0.581 (0.029)**	0.110 (0.708)	−0.141 (0.630)
E^t_{nodal}(LING.R)	−0.013 (0.965)	0.330 (0.249)	**−0.532 (0.047)**	0.192 (0.510)	−0.116 (0.692)
E^t_{nodal}(MOG.L)	−0.287 (0.320)	0.444 (0.111)	**−0.642 (0.013)**	−0.059 (0.842)	−0.267 (0.357)
E^t_{nodal}(PCUN.R)	−0.397 (0.160)	0.426 (0.129)	**−0.802 (<0.001)***	−0.107 (0.716)	−0.400 (0.157)
E^t_{nodal}(TPOmid.L)	−0.256 (0.377)	−0.034 (0.907)	**−0.711 (0.004)***	−0.200 (0.494)	**−0.562 (0.036)**

Note: PANSS, Positive and Negative Symptom Scale; *Indicates correlation survived FDR (false discovery rate) threshold at $q < 0.05$. The partial correlation coefficients were estimated via multiple linear regressions with age, gender, age-by-gender interaction, and medication dosage as covariates. Significant correlation ($P < 0.05$) was indicated by the bold text. For the abbreviations of the cortical regions, see supplementary table 1.

The discrepancies could stem from the different analytical frameworks used in this study and previous work, that is a temporal distance-based estimation on highly sparse dynamic FC backbone in this study in comparison with variance analysis of static graph theoretical metrics in snapshot networks in the works of Du et al and Yu et al.[25,26] Initial exploration of the origins of dynamic FC showed direct relevance between the prominent and stable dynamic FC and underlying anatomical connections[24,56,57] and highlight a rich-club (highly interconnected hubs in structural brain networks) core where functional connections exhibited greatest stability over time to facilitate the dynamic spreading.[56,58] It is noteworthy that convergent evidences have demonstrated a widely spread significantly reduced anatomical connectivity[59,60] and a disrupted rich-club organization in patients with schizophrenia.[61,62] Thus, we speculate the higher fluctuations of dynamic brain network backbone may be attributable to a relaxation of the normal constraints imposed by anatomical interactions. In line with our observation, Ma et al[28] utilized independent vector analysis of time-varying spatial brain connectivity and revealed significantly more fluctuations of spatial concordance in patients with schizophrenia. According to Zalesky et al,[36] dynamic fluctuations in FC appear to be coordinated across the brain so as to realize globally coordinated variations in network efficiency over time, which might represent a balance between optimizing information processing and minimizing metabolic expenditure. However, excessive variability of dynamic FC may prevent thoughts from developing meaningful interconnectedness among successive mental states.[63] Therefore, the higher fluctuations of dynamic brain network backbone revealed here may represent less optimal information processing and an aberration of maintaining the economy metabolic cost in schizophrenia.

Conceptually, temporal nodal efficiency is a measure of localized temporal information transmission. Therefore, it seems plausible that profoundly higher temporal nodal efficiency in the left frontal, right medial parietal, and bilateral subcortical areas may indicate more fluctuations of dynamic FC linking the areas. Of note, the structural aberrations of these areas have been repeatedly revealed in previous neuroimaging studies.[14] For instance, in one recent meta-study, Ellison-Wright and Bullmore[59] found significant reductions in a left frontal–thalamocortical circuit and a temporal network interconnecting the frontal lobe, insula, hippocampus–amygdala, and temporal and occipital lobes. Meanwhile, pathology of subcortical regions has been consistently implicated as robust findings in the pathogenesis of schizophrenia and relationship with various clinical manifestations.[64] The restricted nature of the anatomical reduction may reflect the greater fluctuations of dynamic functional connections in the localized brain regions of patients with schizophrenia as observed in this work. In terms of the functional architecture of the brain,[65] these regions belong to default mode, salience, and frontoparietal subnetworks. According to Christoff et al,[63] thought is constrained automatically by default mode network and deliberately by frontoparietal network, where the modulation is conducted via salience network. Therefore, the significantly higher temporal regional properties may represent a dysregulation of both automatic and deliberate constraints, which contribute to the "profound disruption of thought" characterized by frequent and abrupt leaps from one topic to another in schizophrenia.[63] More importantly, we found that the aberrations of temporal nodal properties were associated with clinical features of schizophrenia in a complex manner. These findings are consistent with the notion that variations in distinct symptom domains arise from alterations of different neural circuits.[66] Of note, given

the uncorrected statistics, the observed significant relationship should be interpreted as exploratory in nature.

In comparison to previous dynamic FC studies of schizophrenia,[19,20,25,26] investigations of the 3D spatiotemporal topology of the temporal brain networks, as in this study, are of important for 2 reasons. First, through incorporating the temporal variations in functional connections into quantitative graph theoretical framework, they allow better appreciation of the intrinsic organization of brain functional networks. Second, the unidirectional characteristic of temporal distance may help to delineate the dynamic reconfiguration of brain networks in prominent cognitive disturbance in schizophrenia, particularly in task-design experiment.[67]

Some issues should be considered when interpreting our findings. First, patients within the study were regularly taking medication during the scan period. Although previous neuroimaging studies have reported pharmacological changes in both localized brain regions and connections in patients with schizophrenia,[68,69] the effects of medication on brain structure and function are far from conclusive.[70] In fact, one recent study suggested that medication is unlikely to be a confounding factor and may on the contrary exert a normalizing influence.[10] We had performed additional analysis to regress the covariant of antipsychotic dose equivalency and found between-group differences intact, suggesting the observed aberrations may reflect the intrinsic disease process rather than the effects of direct pharmacological treatment. Second, a widely used proportional thresholding approach[41,42] was used in this work to retain the dynamic FC backbone. Most recently, van den Heuvel et al[71] performed a case–control study to investigate the influence of proportional thresholding in resting-state fMRI FC and suggested that cautious application of thresholding approach for patient–control comparisons should take into account of potential influence of overall FC. According to van den Heuvel et al,[71] we performed two additional analyses to address this issue. The overall FC strength of the dynamic brain network backbone was initially compared between both groups, where no significant between-group difference was revealed (supplementary figure S2B). Moreover, in following statistical analysis of temporal network metrics, we regressed out potential effects of the overall strength of FC and found consistent between-group differences. As there is no current consensus on the selection of network thresholds in graph theoretical analysis, new advances in thresholding of functional connectomes[72] are therefore expected. Alternative effort may also be made to extend the temporal efficiency metrics into weighted temporal brain network.[73] Third, to date, most fMRI-based dynamic FC studies including the present work are concerned with the changes that happen over the course of seconds.[16,18] Nevertheless, the organization of brain functional networks exhibits temporal dynamics on multiple timescales. For instance, transient cognitive networks established and dissolved on a subsecond timescale.[74] New advances in temporal network construction utilizing neuroimaging techniques with higher temporal resolution (ie, electroencephalography/magnetoencephalography) are therefore of interest to reveal dynamic reconfiguration of networks in prominent cognitive disturbance in schizophrenia at fine timescale.[73,75] Finally, to increase the credibility of the current work, we used 2 independent datasets and mainly focused on the interpretation of the comparable findings. Although this is an advantage of the study, the included patients subsequently have different scanning settings and heterogeneous clinical characteristics. Given the paucity of research in schizophrenia-related dynamic dysconnectivity, further studies with a larger independent study sample are recommended to confirm our observations.

In summary, quantitative assessment of the dynamic FC in terms of temporal small-world properties, as performed in this study, provides the first opportunity to investigate the impaired spatiotemporal topology of the temporal brain networks in schizophrenia. We show that beyond a prominent temporal small-world architecture, there are aberrations of dynamic FC both globally and regionally in schizophrenia, which are also correlated with clinical features. These findings extend the dysconnectivity hypothesis in schizophrenia[2] from static to dynamic brain network and provide insights into the aberrant brain dynamics, which may help unravel the pathophysiologic mechanisms of the disease.

Supplementary Material

Supplementary data are available at *Schizophrenia Bulletin* online.

Funding

This work was supported by the Fundamental Research Funds for the Central Universities (2018QNA5017 to Y.S.), by Zhejiang University under 'Hundred Talents Programs' (to Y.S.), by the National Healthcare Group (NHG 11003 & 12003 to K.S.), and by the A*STAR/Singapore Bioimaging Consortium (ASTAR/SBIC 009/2006 to K.S.).

Acknowledgement

The authors declared no potential conflict of interest with respect to the authorship and publication of this article.

Appendix

Appendix Table. Glossary of key concepts used in this article

Name	Measurement and Meaning
Node	Corresponding to the region of interest defined using parcellation atlas and it is constant in the snapshot static graph at each sliding-window.
Contact	Connection linking a pair of nodes in the snapshot static graphs at each sliding-window.
Sparsity	The ratio of the number of existing contacts divided by the maximum possible number of contacts in the snapshot static graphs.
Aggregated network	Aggregate the contacts over the entire network lifetime, ie, a connection between a pair of nodes would be determined to exist if the pair of nodes is linked by at least one contact at any time step.
Edge	Connection linking a pair of nodes in the aggregated network.
Temporal distance ($\tau_{i\to j}(t)$)	$\tau_{i\to j}(t)$ is defined as the smallest number of time steps required to reach node j from node i starting at time t. Temporal distance is a measure in the time domain, with the smallest value being 1 (when i and j are connected through a static path at time t irrespective of the geometric distance of the static path) and the largest value being infinity (when no time-respecting path exists from i to j at time t.
Temporal global efficiency (E^t_{glob})	E^t_{glob} measures how efficient the overall information is exchanged in a time-varying system.
Temporal local efficiency (E^t_{loc})	E^t_{loc} measures the overall resilience of the temporal network to local failures caused by the removal of any node at any time step.
Temporal nodal efficiency ($E^t_{nodal}(G, i)$)	$E^t_{nodal}(G, i)$ measures the ability of temporal information transmission of node i in the temporal network: a node with high $E^t_{nodal}(G, i)$ indicates greater interconnectivity with other nodes in the temporal network.

References

1. Howes OD, Murray RM. Schizophrenia: an integrated sociodevelopmental-cognitive model. *Lancet*. 2014;383:1677–1687.
2. Friston K, Brown HR, Siemerkus J, Stephan KE. The dysconnection hypothesis (2016). *Schizophr Res*. 2016;176:83–94.
3. Pettersson-Yeo W, Allen P, Benetti S, McGuire P, Mechelli A. Dysconnectivity in schizophrenia: where are we now? *Neurosci Biobehav Rev*. 2011;35:1110–1124.
4. Bullmore ET, Frangou S, Murray RM. The dysplastic net hypothesis: an integration of developmental and dysconnectivity theories of schizophrenia. *Schizophr Res*. 1997;28:143–156.
5. Stephan KE, Friston KJ, Frith CD. Dysconnection in schizophrenia: from abnormal synaptic plasticity to failures of self-monitoring. *Schizophr Bull*. 2009;35:509–527.
6. Bullmore E, Sporns O. Complex brain networks: graph theoretical analysis of structural and functional systems. *Nat Rev Neurosci*. 2009;10:186–198.
7. Sporns O. The human connectome: a complex network. *Ann N Y Acad Sci*. 2011;1224:109–125.
8. Liu Y, Liang M, Zhou Y, et al. Disrupted small-world networks in schizophrenia. *Brain*. 2008;131:945–961.
9. Yu Q, Sui J, Rachakonda S, et al. Altered topological properties of functional network connectivity in schizophrenia during resting state: a small-world brain network study. *PLoS One*. 2011;6:e25423.
10. Rubinov M, Knock SA, Stam CJ, et al. Small-world properties of nonlinear brain activity in schizophrenia. *Hum Brain Mapp*. 2009;30:403–416.
11. Alexander-Bloch AF, Gogtay N, Meunier D, et al. Disrupted modularity and local connectivity of brain functional networks in childhood-onset schizophrenia. *Front Syst Neurosci*. 2010;4:147.
12. Sun Y, Dai Z, Li J, Collinson SL, Sim K. Modular-level alterations of structure-function coupling in schizophrenia connectome. *Hum Brain Mapp*. 2017;38:2008–2025.
13. Lynall ME, Bassett DS, Kerwin R, et al. Functional connectivity and brain networks in schizophrenia. *J Neurosci*. 2010;30:9477–9487.
14. Fornito A, Zalesky A, Pantelis C, Bullmore ET. Schizophrenia, neuroimaging and connectomics. *Neuroimage*. 2012;62:2296–2314.
15. van den Heuvel MP, Fornito A. Brain networks in schizophrenia. *Neuropsychol Rev*. 2014;24:32–48.
16. Hutchison RM, Womelsdorf T, Allen EA, et al. Dynamic functional connectivity: promise, issues, and interpretations. *Neuroimage*. 2013;80:360–378.
17. Calhoun VD, Miller R, Pearlson G, Adalı T. The chronnectome: time-varying connectivity networks as the next frontier in fMRI data discovery. *Neuron*. 2014;84:262–274.
18. Preti MG, Bolton TA, Van De Ville D. The dynamic functional connectome: state-of-the-art and perspectives. *Neuroimage*. 2016;160:41–54.
19. Sakoğlu U, Pearlson GD, Kiehl KA, Wang YM, Michael AM, Calhoun VD. A method for evaluating dynamic functional network connectivity and task-modulation: application to schizophrenia. *MAGMA*. 2010;23:351–366.
20. Damaraju E, Allen EA, Belger A, et al. Dynamic functional connectivity analysis reveals transient states of dysconnectivity in schizophrenia. *Neuroimage Clin*. 2014;5:298–308.
21. Miller RL, Yaesoubi M, Turner JA, et al. Higher dimensional meta-state analysis reveals reduced resting fMRI connectivity dynamism in schizophrenia patients. *PLoS One*. 2016;11:e0149849.
22. Su J, Shen H, Zeng LL, Qin J, Liu Z, Hu D. Heredity characteristics of schizophrenia shown by dynamic functional connectivity analysis of resting-state functional MRI scans of unaffected siblings. *Neuroreport*. 2016;27:843–848.
23. Betzel RF, Fukushima M, He Y, Zuo XN, Sporns O. Dynamic fluctuations coincide with periods of high and low modularity in resting-state functional brain networks. *Neuroimage*. 2016;127:287–297.

24. Liégeois R, Ziegler E, Phillips C, et al. Cerebral functional connectivity periodically (de)synchronizes with anatomical constraints. *Brain Struct Funct*. 2016;221:2985–2997.
25. Du Y, Pearlson GD, Yu Q, et al. Interaction among subsystems within default mode network diminished in schizophrenia patients: a dynamic connectivity approach. *Schizophr Res*. 2016;170:55–65.
26. Yu Q, Erhardt EB, Sui J, et al. Assessing dynamic brain graphs of time-varying connectivity in fMRI data: application to healthy controls and patients with schizophrenia. *Neuroimage*. 2015;107:345–355.
27. Dai Z, Chen Y, Li J, Fam J, Bezerianos A, Sun Y. Temporal efficiency evaluation and small-worldness characterization in temporal networks. *Sci Rep*. 2016;6:34291.
28. Ma S, Calhoun VD, Phlypo R, Adalı T. Dynamic changes of spatial functional network connectivity in healthy individuals and schizophrenia patients using independent vector analysis. *Neuroimage*. 2014;90:196–206.
29. Yan CG, Zang YF. DPARSF: a MATLAB toolbox for "Pipeline" data analysis of resting-state fMRI. *Front Syst Neurosci*. 2010;4:13.
30. Ashburner J. A fast diffeomorphic image registration algorithm. *Neuroimage*. 2007;38:95–113.
31. Power JD, Barnes KA, Snyder AZ, Schlaggar BL, Petersen SE. Spurious but systematic correlations in functional connectivity MRI networks arise from subject motion. *Neuroimage*. 2012;59:2142–2154.
32. Woods SW. Chlorpromazine equivalent doses for the newer atypical antipsychotics. *J Clin Psychiatry*. 2003;64:663–667.
33. Kay SR, Fiszbein A, Opler LA. The positive and negative syndrome scale (PANSS) for schizophrenia. *Schizophr Bull*. 1987;13:261–276.
34. Allen EA, Damaraju E, Plis SM, Erhardt EB, Eichele T, Calhoun VD. Tracking whole-brain connectivity dynamics in the resting state. *Cereb Cortex*. 2014;24:663–676.
35. Hutchison RM, Womelsdorf T, Gati JS, Everling S, Menon RS. Resting-state networks show dynamic functional connectivity in awake humans and anesthetized macaques. *Hum Brain Mapp*. 2013;34:2154–2177.
36. Zalesky A, Fornito A, Cocchi L, Gollo LL, Breakspear M. Time-resolved resting-state brain networks. *Proc Natl Acad Sci USA*. 2014;111:10341–10346.
37. Tzourio-Mazoyer N, Landeau B, Papathanassiou D, et al. Automated anatomical labeling of activations in SPM using a macroscopic anatomical parcellation of the MNI MRI single-subject brain. *Neuroimage*. 2002;15:273–289.
38. Zalesky A, Fornito A, Bullmore E. On the use of correlation as a measure of network connectivity. *Neuroimage*. 2012;60:2096–2106.
39. Shirer WR, Ryali S, Rykhlevskaia E, Menon V, Greicius MD. Decoding subject-driven cognitive states with whole-brain connectivity patterns. *Cereb Cortex*. 2012;22:158–165.
40. Zalesky A, Breakspear M. Towards a statistical test for functional connectivity dynamics. *Neuroimage*. 2015;114:466–470.
41. Achard S, Bullmore E. Efficiency and cost of economical brain functional networks. *PLoS Comput Biol*. 2007;3:e17.
42. Bassett DS, Bullmore E, Verchinski BA, Mattay VS, Weinberger DR, Meyer-Lindenberg A. Hierarchical organization of human cortical networks in health and schizophrenia. *J Neurosci*. 2008;28:9239–9248.
43. Pan RK, Saramäki J. Path lengths, correlations, and centrality in temporal networks. *Phys Rev E Stat Nonlin Soft Matter Phys*. 2011;84:016105.
44. Holme P. Analyzing temporal networks in social media. *Proc IEEE*. 2014;102:1922–1933.
45. Holme P. Modern temporal network theory: a colloquium. *Eur Phys J B*. 2015;88:1–30.
46. Holme P, Saramäki J. Temporal networks. *Phys Rep*. 2012;519:97–125.
47. Watts DJ, Strogatz SH. Collective dynamics of 'small-world' networks. *Nature*. 1998;393:440–442.
48. Nichols TE, Holmes AP. Nonparametric permutation tests for functional neuroimaging: a primer with examples. *Hum Brain Mapp*. 2002;15:1–25.
49. Wang J, Wang L, Zang Y, et al. Parcellation-dependent small-world brain functional networks: a resting-state fMRI study. *Hum Brain Mapp*. 2009;30:1511–1523.
50. de Reus MA, van den Heuvel MP. The parcellation-based connectome: limitations and extensions. *Neuroimage*. 2013;80:397–404.
51. Makris N, Meyer JW, Bates JF, Yeterian EH, Kennedy DN, Caviness VS. MRI-based topographic parcellation of human cerebral white matter and nuclei II. Rationale and applications with systematics of cerebral connectivity. *Neuroimage*. 1999;9:18–45.
52. Kennedy DN, Lange N, Makris N, Bates J, Meyer J, Caviness VS Jr. Gyri of the human neocortex: an MRI-based analysis of volume and variance. *Cereb Cortex*. 1998;8:372–384.
53. Craddock RC, James GA, Holtzheimer PE III, Hu XP, Mayberg HS. A whole brain fMRI atlas generated via spatially constrained spectral clustering. *Hum Brain Mapp*. 2012;33:1914–1928.
54. Leonardi N, Van De Ville D. On spurious and real fluctuations of dynamic functional connectivity during rest. *Neuroimage*. 2015;104:430–436.
55. Bassett DS, Nelson BG, Mueller BA, Camchong J, Lim KO. Altered resting state complexity in schizophrenia. *Neuroimage*. 2012;59:2196–2207.
56. Shen K, Hutchison RM, Bezgin G, Everling S, McIntosh AR. Network structure shapes spontaneous functional connectivity dynamics. *J Neurosci*. 2015;35:5579–5588.
57. Deco G, Jirsa VK, McIntosh AR. Emerging concepts for the dynamical organization of resting-state activity in the brain. *Nat Rev Neurosci*. 2011;12:43–56.
58. van den Heuvel MP, Sporns O. Rich-club organization of the human connectome. *J Neurosci*. 2011;31:15775–15786.
59. Ellison-Wright I, Bullmore E. Meta-analysis of diffusion tensor imaging studies in schizophrenia. *Schizophr Res*. 2009;108:3–10.
60. Fitzsimmons J, Kubicki M, Shenton ME. Review of functional and anatomical brain connectivity findings in schizophrenia. *Curr Opin Psychiatry*. 2013;26:172–187.
61. van den Heuvel MP, Sporns O, Collin G, et al. Abnormal rich club organization and functional brain dynamics in schizophrenia. *JAMA Psychiatry*. 2013;70:783–792.
62. Collin G, Kahn RS, de Reus MA, Cahn W, van den Heuvel MP. Impaired rich club connectivity in unaffected siblings of schizophrenia patients. *Schizophr Bull*. 2014;40:438–448.
63. Christoff K, Irving ZC, Fox KC, Spreng RN, Andrews-Hanna JR. Mind-wandering as spontaneous thought: a dynamic framework. *Nat Rev Neurosci*. 2016;17:718–731.

64. Rimol LM, Hartberg CB, Nesvåg R, et al. Cortical thickness and subcortical volumes in schizophrenia and bipolar disorder. *Biol Psychiatry*. 2010;68:41–50.
65. Smith SM, Fox PT, Miller KL, et al. Correspondence of the brain's functional architecture during activation and rest. *Proc Natl Acad Sci USA*. 2009;106:13040–13045.
66. Meyer-Lindenberg A, Weinberger DR. Intermediate phenotypes and genetic mechanisms of psychiatric disorders. *Nat Rev Neurosci*. 2006;7:818–827.
67. Braun U, Schäfer A, Walter H, et al. Dynamic reconfiguration of frontal brain networks during executive cognition in humans. *Proc Natl Acad Sci USA*. 2015;112:11678–11683.
68. Ho BC, Andreasen NC, Ziebell S, Pierson R, Magnotta V. Long-term antipsychotic treatment and brain volumes: a longitudinal study of first-episode schizophrenia. *Arch Gen Psychiatry*. 2011;68:128–137.
69. Vita A, De Peri L, Deste G, Barlati S, Sacchetti E. The effect of antipsychotic treatment on cortical gray matter changes in schizophrenia: does the class matter? A meta-analysis and meta-regression of longitudinal magnetic resonance imaging studies. *Biol Psychiatry*. 2015;78:403–412.
70. Goff DC, Falkai P, Fleischhacker WW, et al. The long-term effects of antipsychotic medication on clinical course in schizophrenia. *Am J Psychiatry*. 2017;174:840–849.
71. van den Heuvel MP, de Lange SC, Zalesky A, Seguin C, Yeo BTT, Schmidt R. Proportional thresholding in resting-state fMRI functional connectivity networks and consequences for patient-control connectome studies: Issues and recommendations. *Neuroimage*. 2017;152:437–449.
72. Váša F, Bullmore ET, Patel AX. Probabilistic thresholding of functional connectomes: application to schizophrenia. *Neuroimage*. 2018;172:326–340.
73. Thompson WH, Brantefors P, Fransson P. From static to temporal network theory: applications to functional brain connectivity. *Network Neurosci*. 2017;1:69–99.
74. Bola M, Sabel BA. Dynamic reorganization of brain functional networks during cognition. *Neuroimage*. 2015;114:398–413.
75. Naim-Feil J, Rubinson M, Freche D, et al. Altered brain network dynamics in schizophrenia: a cognitive electroencephalography study. *Biol Psychiatry Cogn Neurosci Neuroimaging*. 2018;3:88–98.